Diurnal modulation of pacemaker potentials and calcium current in the mammalian circadian clock

Cyriel M. A. Pennartz, Marcel T. G. de Jeu, Nico P. A. Bos, Jeroen Schaap & Alwin M. S. Geurtsen

Graduate School Neurosciences Amsterdam, Netherlands Institute for Brain Research, Meibergdreef 33, 1105 AZ, Amsterdam, The Netherlands

The central biological clock of the mammalian brain is located in the suprachiasmatic nucleus. This hypothalamic region contains neurons that generate a circadian rhythm on a single-cell basis. Clock cells transmit their circadian timing signals to other brain areas by diurnal modulation of their spontaneous firing rate. The intracellular mechanism underlying rhythm generation is thought to consist of one or more self-regulating molecular loops, but it is unknown how these loops interact with the plasma membrane to modulate the ionic conductances that regulate firing behaviour. Here we demonstrate a diurnal modulation of Ca^{2+} current in suprachiasmatic neurons. This current strongly contributes to the generation of spontaneous oscillations in membrane potential, which occur selectively during daytime and are tightly coupled to spike generation. Thus, day–night modulation of Ca^{2+} current is a central step in transducing the intracellular cycling of molecular clocks to the rhythm in spontaneous firing rate.

It has long been known that neurons in the suprachiasmatic nucleus (SCN) transmit circadian output to other brain areas by diurnal modulation of their spontaneous discharge frequency[1–5]. When firing activity of SCN neurons is monitored in cultures of dissociated cells, many of them express a circadian rhythm that is asynchronous with that of other cells, indicating the cell-autonomous nature of the oscillator[4]. The molecular loops operating within clock cells involve transcription, translation and negative protein-mediated feedback on gene expression[5,6]. Much less is known about the signals by which the core loop communicates with ionic channels and transporters in the plasma membrane, which directly regulate membrane excitability. Ionic channels may be under direct transcriptional control of the core loop or, alternatively, may be regulated by as-yet unidentified clock-controlled genes[5,6]. A principal step in the elucidation of this problem is to dissect the ionic mechanisms by which the circadian message from the molecular clock is transduced into bioelectric output. This, however, is not a simple problem. First, there are many ionic currents in the SCN that may be targeted by the molecular clock[7–10], yet their contribution to spontaneous firing is largely unknown. Second, ionic currents in SCN neurons can be monitored by patch-clamp recordings for several hours[10], which is, however, too short to study circadian modulation within a single neuron. This technical limitation necessitates groupwise comparisons between neurons recorded during different circadian phases. This consideration, combined with the finding that clock cells become desynchronized in dissociated-cell cultures[4], led us to use acutely prepared brain slices in studying diurnal modulation of ionic conductances. Before investigating specific conductances, however, we assessed day–night differences in integrated electrophysiological behaviour of SCN cells, which can be optimally studied with the use of perforated patch recordings in current clamp mode[10].

Oscillations in membrane potential

We first verified whether our preparation was capable of expressing a circadian rhythm in firing. Indeed, the spontaneous firing rate (SFR) was higher in neurons recorded during day (8.3 ± 0.6 Hz, mean ± s.e.m.; $n = 51$) than in the night (2.5 ± 0.5 Hz, $n = 36$) ($P < 1 \times 10^{-6}$; compare with refs 2, 4). We next asked whether diurnal differences in membrane properties would be detectable in the absence of firing activity. After spiking was abolished by tetrodotoxin (TTX; 1 μM), we observed two dramatic day–night differences: day cells ($n = 41$) were strongly and tonically depolarized with respect to night cells ($n = 21$) (compare with ref. 10) and exhibited membrane potential oscillations at a frequency of 2–7 Hz that were absent in night cells (Fig. 1). The time-averaged membrane potentials were -43 ± 1 and -55 ± 1 mV for the day and night phases, respectively ($P < 1 \times 10^{-6}$). This difference was associated with an enhanced input resistance during the day (2.3 ± 0.1 GΩ) compared with the night (1.3 ± 0.2 GΩ) ($P < 5 \times 10^{-5}$). The mean frequency and peak-to-valley amplitude of the oscillations were respectively 4.0 ± 0.3 Hz and 14 ± 1 mV during the day ($n = 41$), whereas clear oscillations were only rarely detectable during the night (mean frequency, 0.4 ± 0.2 Hz; amplitude, 1 ± 1 mV; $n = 21$) (both $P < 1 \times 10^{-6}$). The fraction of day cells showing oscillations (37 of 41 cells; 90%) was significantly larger than that during the night (3 of 21 cells; 15%) ($P < 5 \times 10^{-9}$). We quantified the relative strength of the oscillations by spectral analysis of membrane potential traces and by computing the ratio of the peak in the power spectrum in the 2–7-Hz frequency band over the power averaged across the 0.5–1.0-Hz band ('peak/basal ratio'). This ratio was dramatically larger during the day (41.4 ± 7.8 mV^2) than the night (2.5 ± 1.5 mV^2) ($P < 1 \times 10^{-6}$). The oscillations displayed a distinct voltage dependence: they became smaller and less regular with depolarization above or hyperpolarization below the range of resting potentials (Fig. 1c). The paucity of oscillations in night cells could not be ascribed to their more hyperpolarized state, because depolarization by current injection failed to induce sustained oscillatory behaviour ($n = 21$; Fig. 1b). The TTX-induced depolarization in day cells (Fig. 1d) could not be attributed to a gradual deterioration of cell quality, because it was selectively found in day but not night cells and because the membrane potential recovered after prolonged TTX washout in all 12 day cells tested (Fig. 1a).

We next examined the ionic mechanism underlying the oscillations occurring during daytime. When we replaced Ca^{2+} with Mg^{2+} in a bathing medium containing TTX, the oscillation was strongly and reversibly reduced, as quantified by the peak/basal ratio ($P < 0.05$, $n = 6$; Fig. 2a). Furthermore, the L-type Ca^{2+} channel blocker nimodipine[11–13] (2 μM) virtually abolished the oscillations ($P < 0.02$, $n = 7$; Fig. 2b). Neither treatment affected the time-averaged membrane potential or input resistance

(Fig. 2e, f). Indeed, in the presence of both TTX and nimodipine the membrane potential during the day (-45 ± 2 mV, $n = 7$) remained significantly different from the night (-54 ± 2 mV, $n = 5$) ($P < 0.05$), and the same applied to the input resistance (day, 2.0 ± 0.2 GΩ; night, 1.2 ± 0.2 GΩ; $P < 0.05$). The suppression of oscillations was also clearly present, albeit less strong, when using a tenfold lower dose of nimodipine (0.2 μM; $n = 3$). In contrast, the oscillations were not affected by the following: 50 μM Ni^{2+}, a preferential low-voltage-activated Ca^{2+} channel blocker[7,11,12,14,15] ($n = 3$); the N-type Ca^{2+} channel blocker ω-conotoxin GVIA[7,11,13] (1 μM; $n = 4$); the P/Q-type Ca^{2+} channel blocker ω-agatoxin IVB[16] (0.2 μM; $n = 4$); and an enhancement of the TTX dose to 10 μM ($n = 3$). First, these results indicate a major role for L-type Ca^{2+} channels in mediating the oscillations. These channels are defined by their relatively long-lasting currents evoked by depolarizing voltage steps[11–14]. Second, the oscillations and tonically depolarized membrane potential during the day are dissociable and should thus be attributed to different ionic mechanisms.

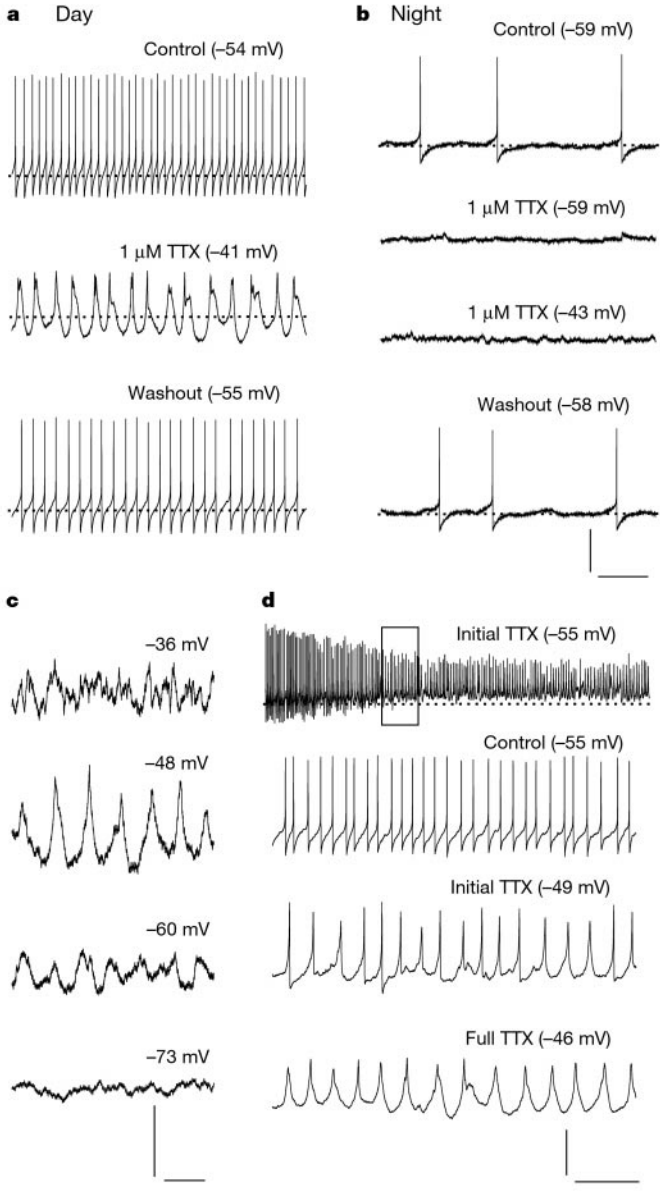

Figure 1 Properties of membrane potential oscillations in SCN. **a**, Day: TTX revealed oscillations and tonically depolarized the membrane. Dotted lines, the time-averaged membrane potential values. **b**, Night: TTX failed to uncover oscillations or depolarize the cell. In the third trace from top, the cell was depolarized by constant current injection. **c**, Voltage dependence of oscillations during TTX. Membrane potential was varied by constant current injection. **d**, Spikes were closely associated with the peak phase of oscillations. The top trace presents the phase of TTX wash-in. Dotted line, membrane potential before TTX. The inset is enlarged in the third trace from the top and represents the mid-phase of TTX wash-in. Calibration bars: **a**, **b**, 40 mV, 500 ms, except middle trace in **a**, 20 mV; **c**, 10 mV, 500 ms; **d**, top, 30 mV, 5000 ms; **d**, second trace, 40 mV, 500 ms; **d**, bottom traces, 20 mV, 500 ms.

L-type calcium current

Led by the observation that no sustained oscillations could be induced in night cells, we predicted that Ca^{2+} currents display a larger amplitude during the day than the night. To test this, we recorded current–voltage relationships in voltage-clamp mode. Thresholds of Ca^{2+} currents were situated at -60 to -50 mV in most cells, with low-threshold (T-type) current being absent or of minor amplitude (Fig. 3; holding potential -90 mV). The decay of Ca^{2+} current was marked by a fast and slow component. Their time constants were not significantly different for the day (τ_1, 15 ± 1 ms; τ_2, 177 ± 13 ms; $n = 20$) and night (τ_1, 16 ± 1 ms; τ_2, 183 ± 27 ms; $n = 21$) (quantified at steps to -20 mV). However, the peak amplitudes were significantly larger during the day (-400 ± 42 pA at -20 mV) than night (-241 ± 30 pA) ($P < 0.01$; Fig. 3d). In addition, the amplitude of the slowly decaying component, as measured 150 ms after step onset, was significantly larger in day cells (-145 ± 19 pA) than in night cells

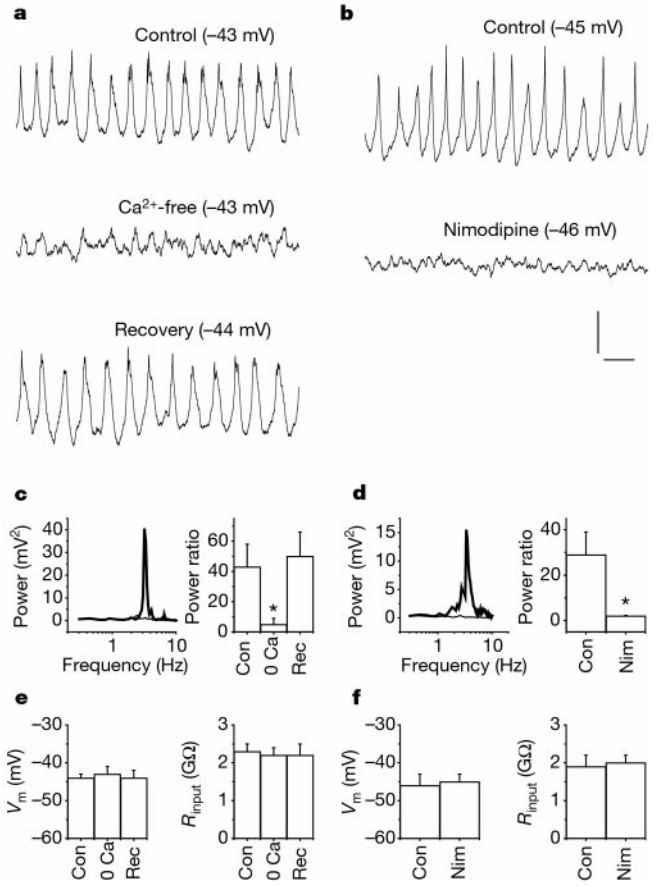

Figure 2 Role of Ca^{2+} channels in mediating daytime oscillations. **a**, Application of Ca^{2+}-free medium reversibly suppressed the oscillations. **b**, Nimodipine (2 μM) also abolished the oscillations. Calibration bars (**a** and **b**), 10 mV, 500 ms. **c**, Power spectrum computed over 30-s traces (left). Thick and thin curves, control and Ca^{2+}-free conditions. Peak/basal ratios of spectral components in control (Con), Ca^{2+}-free medium (0 Ca; asterisk, $P < 0.05$) and recovery (Rec) (right). **d**, As for **c**, but for nimodipine (Nim) (asterisk, $P < 0.02$). **e**, **f**, Lack of significant changes in membrane potential (V_m) and input resistance (R_{input}) in Ca^{2+}-free medium (**e**) or nimodipine (**f**).

(−72 ± 11 pA) ($P < 0.002$). A similar day–night difference was found when using a holding potential of −70 mV, making a contribution by T-type Ca^{2+} channels unlikely[7,11,12,14]. These differences could not be attributed to a difference in cell capacitance (day, 10.3 ± 1.0 pF; night, 8.9 ± 0.8 pF; not significant) or in the voltage dependence of current inactivation. In line with the suppressive effect of nimodipine on daytime oscillations, we found a larger effect of this compound (2 μM) on Ca^{2+} currents during the day than the night. Nimodipine strongly reduced the peak of Ca^{2+} current during the day ($P < 0.01$, $n = 9$), whereas the effect at night was modest ($P < 0.05$, $n = 9$) (Fig. 3e–k). When the amount by which nimodipine reduced the peak current was calculated as a percentage of control, the reduction was stronger for the day (38 ± 5%) than the night (19 ± 3%) ($P < 0.02$). Similarly, the slowly decaying component was attenuated more strongly during the day (35 ± 6%) than the night (14 ± 4%) ($P < 0.02$). Notably, the effect of nimodipine was already visible at voltage levels as low as −50 mV (Fig. 3f; $n = 5$). During nimodipine, a significant day–night difference in Ca^{2+} current remained visible (day, − 236 ± 44 pA; night, −122 ± 24 pA; $P < 0.01$; peak values at −20 mV).

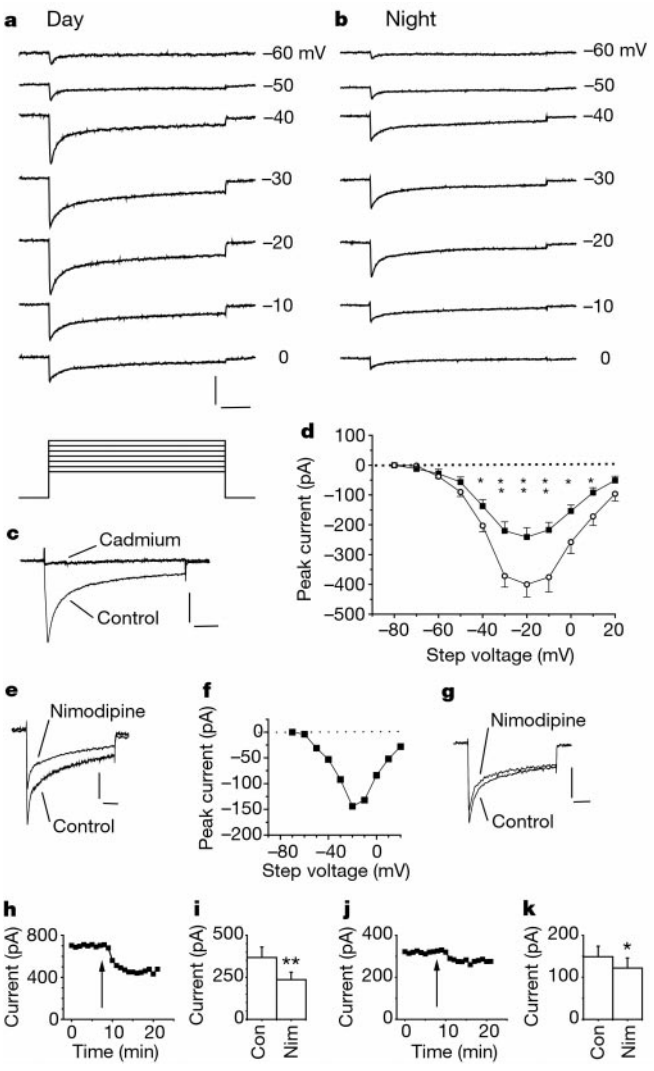

Figure 3 Diurnal modulation of Ca^{2+} current in SCN. **a**, **b**, Activation curves for day and night cells. **c**, Block of Ca^{2+} current by 200 μM Cd^{2+}. **d**, Averaged activation curves for day (open circles) and night (filled squares). Asterisk, $P < 0.05$; double asterisk, $P < 0.01$. **e**, **g**, Effect of nimodipine (2 μM) on Ca^{2+} current during the day (**e**) and night (**g**). **f**, Activation curve of the nimodipine-sensitive component of Ca^{2+} current. **h**, Time course of peak current in the same experiment as **e**. Arrow, onset of nimodipine application. **i**, Effect of nimodipine on peak Ca^{2+} current during day. **j**, **k**, As for **h** and **i**, but during the night. Calibration bars: **a**, **b**, 200 pA, 50 ms; **c**, **e**, 150 pA, 50 ms; **g**, 100 pA, 50 ms.

Regulation of spontaneous firing

We wondered about the relevance of the L-type Ca^{2+} current and the oscillations to which it contributes for the regulation of spontaneous firing in SCN neurons. A first indication for their importance was derived from the initial wash-in phase of our TTX experiments (Fig. 1d; $n = 9$), when spikes were not yet fully blocked but the underlying oscillations were already apparent. Attenuated spikes were consistently observed during the peak but not valley phase of the oscillations. Second, the spontaneous firing rate of day neurons in control medium was positively correlated to their oscillation frequency as measured during TTX (correlation coefficient $r = 0.69$, $P < 5 \times 10^{-6}$, $n = 41$; for the overall population of cells, $r = 0.82$, $P < 1 \times 10^{-6}$, $n = 62$). Third, when we tested the effect of nimodipine on spontaneous firing, we found that the firing rate, spike amplitude and amplitude of the spike afterhyperpolarization (compare with ref. 17) decreased in day ($n = 6$; all $P < 0.05$) but not night cells ($n = 6$) (Fig. 4). These findings suggest that L-type Ca^{2+} current contributes to robust patterning of spikes and ensuing afterhyperpolarizations. Accordingly, we propose that the oscillatory potentials emerging during TTX treatment are considered pacemaker potentials in the sense that they drive and temporally organize spontaneous firing in the presence of functioning Na^+ channels. The effect of nimodipine on spike amplitude may be attributed to a relative lack of Na^+ channel deinactivation due to diminished afterhyperpolarizations between successive spikes, in combination with the tonically depolarized membrane potential during daytime (compare with ref. 7).

Discussion

Our results demonstrate a robust day–night difference in L-type Ca^{2+} current in rat SCN, and thus constitute, to our knowledge, the first evidence for diurnal regulation of intrinsic ionic currents in mammals. L-type Ca^{2+} current contributes to robust, high-frequency firing during daytime and is therefore likely to function as a crucial intermediate between the intracellular molecular clock and the bioelectric output of the SCN, which drives and synchronizes circadian rhythms in the brain and body. Previously, a pioneering study in retinal cells of the mollusc *Bulla gouldiana*[18] reported circadian modulation of a K^+ current regulating the basal membrane potential. With regard to vertebrates, a day–night modulation was shown to occur in a mixed cationic current in cultured chick pineal cells[19], but a causal link between this current and spike activity or melatonin release was not demonstrated, and the avian pineal system differs from the mammalian circadian system in a fundamental way[20]. Our findings suggest how diurnal modulation of Ca^{2+} current contributes to the circadian rhythm in firing rate: Ca^{2+} current mediates the rising phase of 2–7-Hz oscillations and thereby provides an excitatory drive for firing, whereas the falling phase is mediated by a K^+ current and may support Na^+ channel deinactivation. Additional data (not shown here) suggest that this K^+ current is sensitive to tetraethylammonium but not to conventional blockers of Ca^{2+}-dependent K^+ current. Our findings do not imply that this current is also diurnally modulated, nor do they exclude involvement of other currents in oscillatory behaviour or in spontaneous firing[8].

The high amplitude and frequency of SCN daytime oscillations makes them unique relative to oscillatory phenomena in other types of neurons, although dopamine cells may show similar behaviour under particular conditions[21]. The dihydropyridine sensitivity of the oscillations is consistent with the sustained nature of L-type current and its relatively negative voltage range of activation (Fig. 3f), also reported in several other preparations[12,22,23] (but see ref.

14). Periodic Ca^{2+} entry through L-type channels is likely to have a significant impact on intracellular Ca^{2+} homeostasis. Indeed it has been reported that the intracellular Ca^{2+} concentration in SCN neurons is higher during the day than night[24]. Periodic Ca^{2+} entry may alter the activation state of Ca^{2+}-dependent enzymes involved in phase shifting[25] and is likely to affect gene expression[26,27].

In parallel with the Ca^{2+} current modulation, our evidence substantiates the existence of a second, functionally dissociable ionic mechanism underlying the membrane depolarization and enhanced input resistance during daytime (see also ref. 10). The importance of this mechanism is underscored by the day–night difference in excitability that remains clearly visible in the presence of nimodipine (Fig. 4a, b). It probably involves a daytime reduction of a tonically active K^+ current that is central in maintaining the membrane potential *per se* and is sensitive to internal Cs^+ but insensitive to tetraethylammonium (data not shown). Regardless of the precise molecular identity of this current, it can be inferred that at least two ionic mechanisms are subject to diurnal modulation. An as-yet unidentified nimodipine-insensitive component of Ca^{2+} current is likely to be modulated as well (Fig. 3i, k). Thus, the intracellular molecular clock exerts divergent effects on multiple ion channel and/or transporter species, acting in concert to generate the circadian rhythm in firing rate. Now that a well-defined ion channel in SCN has been identified as a target for diurnal modulation, the underlying mechanism can be investigated. The day–night difference in amplitude of the L-type Ca^{2+} current may result from a diurnal change in transcription or translation[5] of Ca^{2+} channel subunits, or in post-translational modifications such as phosphorylation[28,29] or binding of cofactors[30]. An important constraint on such changes is defined by our finding that neither the decay kinetics nor the voltage dependence of Ca^{2+} current were markedly altered. □

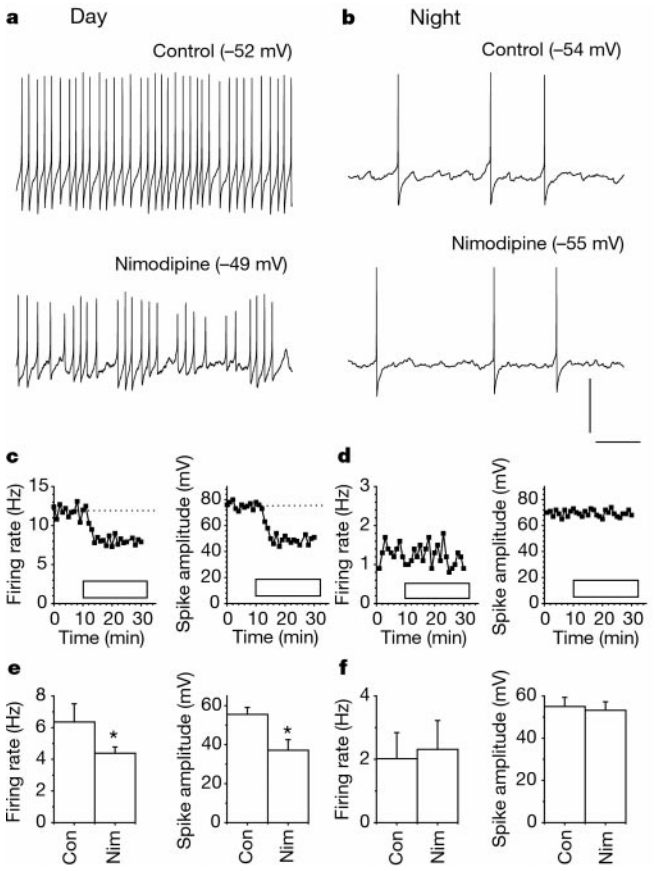

Figure 4 Differential effect of nimodipine on spontaneous firing of SCN neurons during the day and night. **a**, Day: nimodipine (2 μM) caused a reduction in spike amplitude, amplitude of the spike afterhyperpolarization and spontaneous firing rate. **b**, Night: nimodipine failed to affect these parameters. Calibration bars (**a**, **b**), 40 mV, 500 ms. **c**, **d**, Time course of nimodipine effects on firing rate and spike amplitude for day (**c**) and night (**d**). Open bar, period of nimodipine application. **e**, **f**, Decrease in firing rate and spike amplitude was significant across the population of day cells (**e**; asterisk, $P < 0.05$) but absent at night (**f**). Amplitude of the spike afterhyperpolarization in day cells decreased from 19 ± 1 mV (control) to 12 ± 1 mV (nimodipine) ($P < 0.05$).

Methods

Slice preparation

Male Wistar rats (150–300 g) were subjected to a 12:12 h light:dark cycle for at least 3 weeks before use. Rats used for subjective night recordings were housed in a reversed light/dark cycle[8,10]. Slices were prepared during the subjective day to prevent phase shifts. The delays between time of preparation and time of recording were similar for day and night. Day cells were recorded between circadian time (CT) 4 and 8 (refs 2, 10) and night cells between CT 13 and 20, with CT 0 corresponding to light onset. The day–night differences described here are unlikely to be due to after-effects of light, because rats from both the day and night group were exposed for at least 3 h to light before preparation. Strictly speaking, however, we cannot fully rule out effects of prolonged, repeated light exposures and therefore prefer to use the term 'diurnal' instead of 'circadian' modulation. Following national guidelines on animal experiments, rats were anaesthetized[8,17] and transcardially perfused with 30–40 ml of ice-cold artificial cerebrospinal fluid (ACSF; composition (in mM): 124.0 NaCl, 3.5 KCl, 1.0 NaH_2PO_4, 26.2 $NaHCO_3$, 1.3 $MgSO_4$, 2.5 $CaCl_2$, 10.0 D(+)-glucose and 0.0125 bicuculline methochloride; gassed with a mixture of 95% O_2 and 5% CO_2; pH 7.4). Transverse slices (200 μm) of hypothalamus were cut with a vibroslicer (Campden Instruments). Flow rate in the recording chamber (32 °C) was 1.5–2.5 ml min^{-1}.

Current clamp recordings

Current clamp recordings were conducted using the perforated patch technique[10]. The pipette solution contained (in mM): 135.0 potassium gluconate, 10.0 KCl, 10.0 Hepes buffer, 0.5 EGTA (pH adjusted to 7.3 with KOH; osmolality 275–285 mOsm kg^{-1}). Gramicidin and amphotericin B were dissolved in dimethylsulphoxide and added to this solution (final concentrations 250 and 5 μg ml^{-1}, respectively). We found that the combination of these substances produced a lower series resistance (28–67 MΩ) than either substance alone, without loss of recording stability. Patch pipettes (4–7 MΩ) were positioned close to SCN neurons under constant positive pressure, using an upright fixed-stage microscope (Axioskop, Zeiss) equipped with a 40× water-immersion lens (numerical aperture 0.75) with Hoffman modulation contrast. After gigaseal (>3 GΩ) formation, perforation was regularly monitored by measuring capacitive current transients evoked by a −20-mV voltage step. Most recordings were made from the dorsomedial SCN, where cluster I neurons are predominant[17]. Voltage traces were acquired at a sampling rate of 20 kHz using an Axopatch-1D or Axoclamp-2B amplifier and analysed with pClamp (version 6.0.4, Axon Instruments). Membrane potential values were determined from the time-averaged readout of the electrode amplifier and corrected for the liquid junction potential (−12 mV). Our criterion for labelling a cell as 'oscillating' was an oscillation peak–valley amplitude of at least 3 mV and a frequency of at least 0.5 Hz. A Hamming window was used to compute power spectra.

Voltage clamp recordings

Ca^{2+} currents in SCN slices were studied in whole-cell mode because it allowed a lower series resistance (11–32 MΩ; 80% compensation) than perforated patch mode. Owing to their very high input resistance, SCN neurons in slices are electrotonically compact[8,9,17] and allow for voltage clamping of Ca^{2+} current. The pipette medium contained (in mM): 115.0 caesium gluconate, 20.0 tetraethylammonium chloride, 10.0 Hepes buffer, 0.5 EGTA, 2.0 $MgCl_2$, 20.0 sodium phosphocreatine, 2.0 Na_2ATP, 0.3 Na_3GTP and 0.1 leupeptin (pH 7.3; osmolality 275–285 mOsm kg^{-1}; pipette resistance 4–7 MΩ). The ACSF contained (in mM): 68.0 NaCl, 3.5 KCl, 1.0 NaH_2PO_4, 26.2 $NaHCO_3$, 1.3 $MgSO_4$, 2.5 $CaCl_2$, 10.0 D(+)-glucose, 60 tetraethylammonium chloride, 3.0 CsCl, 5.0 4-aminopyridine, 0.0125 bicuculline and 0.001 tetrodotoxin (pH 7.4). Ca^{2+} instead of Ba^{2+} was used as charge carrier because Ca^{2+}-dependent inactivation of Ca^{2+} current may be subject to diurnal modulation and is thus interesting to take into account. Currents were filtered at 1–2 kHz and digitized every 100–200 μs using an Axopatch-1D amplifier. Corrections were made for the liquid junction potential (−9 mV). Cells were accepted for analysis when two criteria indicative of good voltage clamp control were satisfied: the current–voltage relationship showed a graded increment in Ca^{2+} current in the range −60 to −20 mV; and the onset of Ca^{2+} current was not delayed with respect to the voltage step. We used a P/4 protocol to subtract leak currents.

Drugs and statistics

All drugs were administered by bath application. Stock solutions were prepared by dissolving nimodipine (RBI) in 100% ethanol and TTX (Alomone Labs), ω-conotoxin GVIA and ω-agatoxin IVB (Peptides International) in distilled water. These solutions were diluted in ACSF to their final concentrations. Nimodipine was protected from light during these procedures. When using ω-agatoxin IVB, the perfusion system was pre-exposed to a 0.01% cytochrome *c* solution to prevent the peptide binding to tubing and containers. The toxin was applied for at least 25 min. $NiCl_2$ was obtained from Sigma. Groups of cells were statistically compared with the use of Mann–Whitney's *U*-test and Wilcoxon's matched-

pairs signed-rank test for unpaired and paired comparisons, respectively. Fisher's exact test was used to evaluate the difference in prevalence of oscillations across populations of day and night cells. Correlation coefficients between firing rates and oscillation frequencies were determined by computing Spearman's rank correlation. All numerical values both in text and graphs represent the mean ± s.e.m.

Received 6 November 2001; accepted 15 February 2002.
Published online 3 March 2002, DOI 10.1038/nature728.

1. Inouye, S.-I. T. & Kawamura, H. Persistence of circadian rhythmicity in a mammalian hypothalamic "island" containing the suprachiasmatic nucleus. *Proc. Natl Acad. Sci. USA* **76,** 5962–5966 (1979).
2. Green, D. J. & Gillette, R. Circadian rhythm of firing rate recorded from single cells in the rat suprachiasmatic brain slice. *Brain Res.* **245,** 198–200 (1982).
3. Schwartz, W. J., Gross, R. A. & Morton, M. T. The suprachiasmatic nuclei contain a tetrodotoxin-resistant circadian pacemaker. *Proc. Natl Acad. Sci. USA* **84,** 1694–1698 (1987).
4. Welsh, D. K., Logothetis, D. E., Meister, M. & Reppert, S. M. Individual neurons dissociated from rat suprachiasmatic nucleus express independently phased circadian firing rhythms. *Neuron* **14,** 697–706 (1995).
5. Reppert, S. M. & Weaver, D. R. Molecular analysis of mammalian circadian rhythms. *Annu. Rev. Physiol.* **63,** 547–676 (2001).
6. Allada, R., Emery, P., Takahashi, J. S. & Rosbash, M. Stopping time: the genetics of fly and mouse circadian clocks. *Annu. Rev. Neurosci.* **24,** 1091–1119 (2001).
7. Huang, R.-C. Sodium and calcium currents in acutely dissociated neurons from rat suprachiasmatic nucleus. *J. Neurophysiol.* **70,** 1692–1703 (1993).
8. Pennartz, C. M. A., Bierlaagh, M. A. & Geurtsen, A. M. S. Cellular mechanisms underlying spontaneous firing in rat suprachiasmatic nucleus: involvement of a slowly inactivating component of sodium current. *J. Neurophysiol.* **78,** 1811–1825 (1997).
9. Jiang, Z.-G., Yang, Y., Liu, Z.-P. & Allen, C. N. Membrane properties and synaptic inputs of suprachiasmatic nucleus neurons in rat brain slices. *J. Physiol. (Lond.)* **499,** 141–159 (1997).
10. De Jeu, M. T. G., Hermes, M. H. L. J. & Pennartz, C. M. A. Circadian modulation of membrane properties in slices of rat suprachiasmatic nucleus. *Neuroreport* **9,** 3725–3729 (1998).
11. Mogul, D. J. & Fox, A. P. Evidence for multiple types of Ca^{2+} channels in acutely isolated hippocampal CA3 neurones of the guinea-pig. *J. Physiol. (Lond.)* **433,** 259–281 (1991).
12. Avery, R. B. & Johnston, D. Multiple channel types contribute to the low-voltage-activated calcium current in hippocampal CA3 pyramidal neurons. *J. Neurosci.* **16,** 5567–5582 (1996).
13. Randall, A. & Tsien, R. W. Pharmacological dissection of multiple types of Ca^{2+} channel currents in rat cerebellar granule neurons. *J. Neurosci.* **15,** 2995–3012 (1995).
14. Fox, A. P., Nowycky, M. C. & Tsien, R. W. Kinetic and pharmacological properties distinguishing three types of calcium currents in chick sensory neurons. *J. Physiol. (Lond.)* **394,** 149–172 (1987).
15. Blaxter, T. J., Carlen, P. L. & Niesen, C. Pharmacological and anatomical separation of calcium currents in rat dentate granule neurons *in vitro*. *J. Physiol. (Lond.)* **412,** 93–112 (1989).
16. Adams, M. E., Mintz, I. M., Reily, M. D., Thanabal, V. & Bean, B. P. Structure and properties of ω-Agatoxin IVB, a new antagonist of P-type calcium channels. *Mol. Pharmacol.* **44,** 681–688 (1993).
17. Pennartz, C. M. A., Geurtsen, A. M. S., De Jeu, M. T. G., Sluiter, A. A. & Hermes, M. H. L. J. Electrophysiological and morphological heterogeneity of neurons in slices of rat suprachiasmatic nucleus. *J. Physiol. (Lond.)* **506,** 775–793 (1998).
18. Michel, S., Geusz, M. E., Zaritsky, J. J. & Block, G. D. Circadian rhythm in membrane conductance expressed in isolated neurons. *Science* **259,** 239–241 (1993).
19. D'Souza, T. & Dryer, S. E. A cationic channel regulated by a vertebrate intrinsic circadian oscillator. *Nature* **382,** 165–167 (1996).
20. Takahashi, J. S. & Zatz, M. Regulation of circadian rhythmicity. *Science* **217,** 1104–1111 (1982).
21. Nedergaard, S., Flatman, J. A. & Engberg, I. Nifedipine- and ω-conotoxin-sensitive Ca^{2+} conductances in guinea-pig substantia nigra pars compacta neurones. *J. Physiol. (Lond.)* **466,** 727–747 (1993).
22. Kasai, H. & Neher, E. Dihydropyridine-sensitive and ω-conotoxin-sensitive calcium channels in a mammalian neuroblastoma-glioma cell line. *J. Physiol. (Lond.)* **448,** 161–188 (1992).
23. Fisher, T. E. & Bourque, C. W. Calcium-channel subtypes in the somata and axon terminals of magnocellular neurosecretory cells. *Trends Neurosci.* **19,** 440–444 (1996).
24. Colwell, C. S. Circadian modulation of calcium levels in cells in the suprachiasmatic nucleus. *Eur. J. Neurosci.* **12,** 571–576 (2000).
25. Block, G. D., Khalsa, S. B. S., McMahon, D. G., Michel, S. & Geusz, M. Biological clocks in the retina: Cellular mechanisms of biological timekeeping. *Int. Rev. Cytol.* **146,** 83–143 (1993).
26. Murphy, T. H., Worley, P. F. & Baraban, J. M. L-type voltage-sensitive calcium channels mediate synaptic activation of immediate early genes. *Neuron* **7,** 625–635 (1991).
27. Dolmetsch, R. E., Xu, K. & Lewis, R. S. Calcium oscillations increase the efficiency and specificity of gene expression. *Nature* **392,** 933–936 (1998).
28. Catterall, W. A. Structure and regulation of voltage-gated Ca^{2+} channels. *Annu. Rev. Cell Dev. Biol.* **16,** 521–555 (2000).
29. Ko, G. Y.-P., Ko, M. L. & Dryer, S. E. Circadian regulation of cGMP-gated cationic channels of chick retinal cones: Erk MAP kinase and Ca^{2+}/calmodulin-dependent protein kinase II. *Neuron* **29,** 255–266 (2001).
30. O'Rourke, B., Backx, P. H. & Marban, E. Phosphorylation-independent modulation of L-type calcium channels by magnesium–nucleotide complexes. *Science* **257,** 245–248 (1992).

Acknowledgements

We thank G. Borst, J. Meijer, T. Mulder, S. Taverna and M. Verhage for their comments on the manuscript and F. Lopes da Silva for his stimulating advice. This work was supported by the Netherlands Organization for Scientific Research (NWO).

Correspondence and requests for materials should be addressed to C.M.A.P. (e-mail: c.pennartz@nih.knaw.nl).